Load Balancing Routing in Three Dimensional Wireless Networks

Fan Li* Siyuan Chen* Yu Wang* Jiming Chen†
*Department of Computer Science, University of North Carolina at Charlotte, Charlotte, North Carolina, USA
†State Key Lab of Industrial Control Technology, Zhejiang University, Hangzhou, China

***Abstract*— Although most existing wireless systems and protocols are based on two-dimensional design, in reality, a variety of networks operate in three-dimensions. The design of protocols for 3D networks is surprisingly more difficult than the design of those for 2D networks. In this paper, we investigate how to design load balancing routing for 3D networks. Most current wireless routing protocols are based on Shortest Path Routing (SPR), where packets are delivered along the shortest route from a source to a destination. However, under uniform communication, shortest path routing suffers from uneven load distribution in the network, such as crowed center effect where the center nodes have more load than the nodes in the periphery. Aim to balance the load, we propose a novel 3D routing method, called *3D Circular Sailing Routing* (CSR), which maps the 3D network onto a sphere and routes the packets based on the spherical distance on the sphere. We describe two mapping methods for CSR and then provide theoretical proofs of their competitiveness compared to SPR. For both proposed methods, we conduct simulations to study their performance in grid and random networks.**

I. Introduction

Wireless networks have been undergoing a revolution that promises a significant impact on society. Most existing wireless systems and protocols are based on two-dimensional design, where all wireless nodes are distributed in a two dimensional (2D) plane. This assumption is somewhat justified for applications where wireless devices are deployed on earth surface and where the height of the network is smaller than the transmission radius of a node. However, 2D assumption may no longer be valid if a wireless network is deployed in space, atmosphere, or ocean, where nodes of a network are distributed over a 3D space and the differences in the third dimension are too large to be ignored. In fact, recent interest in wireless sensor networks hints at the strong need to design 3D wireless networks.

Routing in wireless networks has been well studied. Most of current routing protocols are based on shortest path algorithm where the packets travel via the shortest path between a source and a destination. Even for the geographical localized routing protocols, such as greedy routing, the packets usually follow the shortest paths when the network is dense and uniformly distributed. Taking the shortest path can achieve smaller delay or traveled distance, however it can also lead uneven distribution of traffic load in a network. By assuming uniform communications, nodes in the center of a network may have heavier traffic than nodes in the periphery since most of the shortest routes go through them. Thus, nodes in the center may run out of their batteries very quickly. This is true in both 2D and 3D networks.

Load balancing routing [1]–[4] for 2D networks has been studied. However, most existing methods [1]–[3] try to dynamically adjust the routes to balance the real time traffic load based on the knowledge of current load distribution (or current remaining energy distribution), which is not very scalable for large wireless networks. Multi-path routing [4] was also used for load balancing. However, [5] showed unless using a very large number of paths, the load distribution is almost the same as single path routing. Recently, routing methods [6]–[8] to avoid the crowed center problem without traffic load information for 2D networks have been studied. [6] proposed a randomized choice between shortest path and routing on inner/outer radii to level the load in a dense network. Both [7] and [8] proposed novel routing techniques to map the 2D network on a sphere and route the packets based on their virtual coordinates on the sphere. Since the communication is uniform, the crowed center effect vanishes due to symmetry (no "center" on the sphere surface) and the load is balanced.

To avoid the uneven load distribution of shortest path routing (SPR), we focus on designing routing protocols for 3D wireless networks which can achieve both small traveled distance and evenly distributed load in the network. Inspired by the idea from [7], [8], we investigate how to map a 3D network onto a sphere, so that we can route packets on the sphere and eliminate the "hot spots" of congestions in 3D networks. Using new mapping methods, our 3D load balancing routing, called *3D Circular Sailing Routing* (CSR), projects wireless nodes in the 3D network on a 3D or 4D sphere and makes the routing decision based on the spherical distance between virtual coordinates on the sphere instead of the Euclidean distance. CSR can be easily implemented based on either SPR or greedy routing. Each node only needs to compute neighbors' spherical coordinates and the computational overhead is negligible. There are no changes to the communication protocol and no any additional communication overhead. By spreading the traffic across the network, CSR can average the energy consumption (*s.t.*, extend the lifespan of the whole

This work of Y. Wang is supported in part by the US National Science Foundation (NSF) under Grant No. CNS-0721666 and funds provided by the University of North Carolina at Charlotte. The work of J. Chen is supported by Nature Science Foundation of China (No.60604029), Specialized Research Fund for the Doctoral Program of Higher Education (No.20050335020), Scientific Research Fund of Zhejiang Provincial Education Department (No.20061345), Nature Science Foundation of Zhejiang Province (Y106384) and the R&D Program of Zhejiang Province (2007c31038).

network) and reduce congestion of hot spots (*s.t.*, reduce wireless collisions).

The contribution of this paper is summarized as follows:

- We propose two projection methods for CSR to map nodes in 3D space on a sphere (Section II). The projection methods guarantee the one-to-one mapping between nodes in 3D networks and virtual nodes on the sphere.
- We theoretically prove the competitiveness of CSR (Section III). We prove that CSR based on the first mapping method can not guarantee the competitiveness, *i.e.*, the total length of its path can be arbitrary larger than the length of the optimal shortest path. However, we prove the CSR based on the second projection method is $\frac{\pi}{2}(1+\epsilon)$-competitive, where ϵ is a constant depended on the size of the sphere and the network. In other words, CSR can guarantee the total distance traveled by packets is constant competitive even in the worst case.
- We conduct extensive simulations on both grid and random networks (Section IV) to evaluate CSR's performance. The results confirm our theoretical analysis.

II. Load-Balanced 3D Circular Sailing Routing

Our 3D Circular Sailing Routing uses one-to-one projection method to map the wireless nodes in 3D networks onto a sphere and route the packets on the sphere.

A. One-to-one Projection Methods

We propose two projection methods to map the nodes in 3D space to a sphere (either a 3D sphere or a 4D sphere). We use $\|mn\|$ and $d(m'n')$ to represent the Euclidean distance between two points m and n and the geodesic shortest distance between two projections m' and n' on the sphere respectively. On a sphere, the geodesics are the great circles. The shortest path from m' to n' on a sphere is given by the shorter arc of the great circle passing through m' and n'.

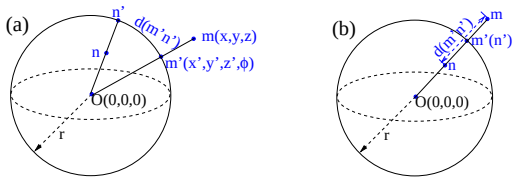

Fig. 1. Projection Method I: from a node $m(x,y,z)$ in 3D space to a node $m'(x',y',z',\phi)$ on the 3D sphere, and two cases for calculation of $d(m'n')$.

Projection Method I: Projection on 3D Sphere. For a 3D wireless network, wireless nodes are distributed in a finite 3D region $\mathbb{R}$ (*e.g.*, a cube). With the information of the network region, we can place the center O of a 3D sphere at the center of the network, whose coordinate is $(0,0,0)$. The radius r of the 3D sphere is an adjustable parameter. Any point $m(x,y,z)$ in $\mathbb{R}$ maps to $m'(x',y',z',\phi)$ on the 3D sphere. Here (x',y',z') is the 3D position of the projection node m', and ϕ is the Euclidean distance from m to the center O. As shown in Fig.1(a), m' is the intersection point of the 3D sphere and line $\overline{mO}$. Sometimes the node is inside the sphere as node n in Fig.1(a). It is easy to show that the virtual coordinates of m' can be computed by the following equations: $x' = \frac{r}{\sqrt{x^2+y^2+z^2}}x$, $y' = \frac{r}{\sqrt{x^2+y^2+z^2}}y$, $z' = \frac{r}{\sqrt{x^2+y^2+z^2}}z$, and $\phi = \sqrt{x^2+y^2+z^2}$. Note that we need to specially deal with the node $O(0,0,0)$ to guarantee that the projection is a one-to-one mapping. Here, we force to map it to the north pole with virtual coordinates $(0,0,r,0)$. To calculate the distance $d(m'n')$ between two projections m' and n', there are two cases as shown in Fig.1. If m' and n' are in different positions on the sphere (Fig.1(a)), $d(m'n')$ is the surface distance on the sphere, which can be computed by $d(m'n') = r\arccos\frac{\|Om'\|^2+\|On'\|^2-\|m'n'\|^2}{2\|Om'\|\|On'\|}$. If m' and n' are at the same point on the sphere (Fig.1(b)), $d(m'n')$ is the Euclidean distance between m and n, *i.e.*, $d(m'n') = \|mn\|$.

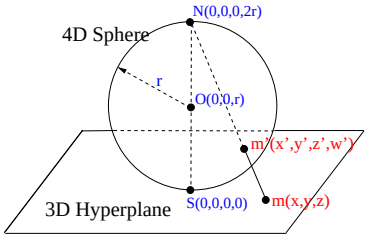

Fig. 2. Projection Method II - Stereographic Projection: an one-to-one mapping from a node m in a 3D hyperplane to a node m' on a 4D sphere.

Projection Method II: Projection on 4D Sphere. In the second projection method, we use *stereographic projection* [9] to map the nodes in 3D networks to a 4D sphere. In projective geometry, stereographic projection is a certain mapping (function) that provides one-to-one mapping between a sphere and a plane. Mapping methods in [7], [8] are actually stereographic projections. Stereographic projection can be extended to high-dimensional space and sphere. Here, we use it to map a 3D region (a 3D hyperplane) on a 4D sphere. A 4D sphere (also called 3-sphere in math), often written as $\mathbb{S}^3$, is the set of points in 4-dimensional Euclidean space which are at distance r from a fixed point of that space. Stereographic projection is conformal in any dimension, i.e., it preserves the angles at which curves cross each other and also preserves circles. Therefore, a circle on the sphere is also a circle in the plane (or hyperplane). As shown in Fig.2, we put a 4D sphere with radius r tangent to the 3D hyperplane at the center of the network. Denote this tangent point as the south pole $S(0,0,0,0)$ of the 4D sphere and its antipodal point as the north pole $N(0,0,0,2r)$. A point $m(x,y,z)$ in the 3D hyperplane is mapped to $m'(x',y',z',w')$ on the 4D sphere, which is the intersection of the line $\overline{mN}$ with the 4D sphere. This provides a one-to-one mapping of the 3D projective hyperplane to a 4D sphere. It is easy to show that the virtual coordinates of m' can be computed by the following equations: $x' = \frac{4r^2x}{x^2+y^2+z^2+4r^2}$, $y' = \frac{4r^2y}{x^2+y^2+z^2+4r^2}$, $z' = \frac{4r^2z}{x^2+y^2+z^2+4r^2}$, $w' = \frac{2r(x^2+y^2+z^2)}{x^2+y^2+z^2+4r^2}$. Geodesics are curves on a surface which give the shortest distance between two points. They are generalization of the concept of a straight

line in the plane. For all spheres, the geodesics are great circles. For any two nodes m and n in 3D network, the geodesic of its projection m' and n' on the 4D sphere is $d(m'n') = r\arccos(\frac{x_{m'}x_{n'}+y_{m'}y_{n'}+z_{m'}z_{n'}+(w_{m'}-r)(w_{n'}-r)}{r^2})$.

B. Routing Algorithm

In circular sailing routing, each node u uses the above projection method (either method I or method II) to compute the virtual coordinates of itself and its neighbors on the sphere. For any link uv, it can calculate the geodesic distance on the sphere between projected nodes u' and v' (*i.e.*, $d(u'v')$). CSR uses $d(u'v')$ as the cost of link uv, and we call it *circular distance*. Then, CSR can apply any general shortest path algorithm with circular distance as the routing metric and choose the route with smallest total circular distance. CSR can also be implemented in a localized fashion and we call it *Localized Circular Sailing Routing* (LCSR). In localized routing, the route decision is made at each node by using only local information. It enjoys low overhead, easy implementation, and good scalability, since it does not need any route discovery and routing table maintenance. Similar to greedy routing, for a current node u, LCSR just forwards the packet to the neighbor v whose projection is the closest to the projection of the destination $\mathbf{t}$ on the sphere, i.e., u forwards the packet to its neighbor v with the minimum $d(v'\mathbf{t}')$.

III. Analysis of Competitiveness

CSR balances the load and eliminates the crowed center effect, but at the same time it uses longer path between the source and the destination than the shortest path. This may increase the total delay of the packet delivery. Therefore, we theoretically study the path length of CSR in this section. Given a routing method $\mathcal{A}$, we define its competitiveness as follows. Let $\mathbf{P}_{\mathcal{A}}(\mathbf{s},\mathbf{t})$ be the path found by $\mathcal{A}$ to connect the source node $\mathbf{s}$ with the target node $\mathbf{t}$. A routing method $\mathcal{A}$ is called *l-competitive* if for every pair of nodes $\mathbf{s}$ and $\mathbf{t}$, the total length of path $\mathbf{P}_{\mathcal{A}}(\mathbf{s},\mathbf{t})$ is within a constant factor l of the length of the shortest path connecting $\mathbf{s}$ and $\mathbf{t}$ in the network. We call l the *competitiveness factor* (CF). We now prove two theorems about the competitiveness of CSR using projection method I and projection method II respectively.

Theorem 1: The distance traveled by CSR with projection method I is not competitive, *i.e.*, it does not have constant CF.

Proof: We prove the theorem by constructing an example where CSR has a arbitrary large CF. See Fig.3 for illustration. The network only has four nodes: $\mathbf{s}$, $\mathbf{t}$, m and n with coordinates $(\epsilon,0,0)$, $(0,\epsilon,0)$, $(0,0,\epsilon)$, and $(\frac{\sqrt{2}}{2}r, \frac{\sqrt{2}}{2}r, 0)$ respectively. Here, ϵ could be an arbitrary small number. The network only has four links: $\mathbf{s}m$, $\mathbf{s}n$, $\mathbf{t}m$, and $\mathbf{t}n$. From $\mathbf{s}$ to $\mathbf{t}$, there are two paths, $\mathbf{s}\to m\to\mathbf{t}$ and $\mathbf{s}\to n\to\mathbf{t}$. Applying the first projection method (Projection Method I), CSR gets the positions of the projected nodes: $\mathbf{s}'(r,0,0,\epsilon)$, $\mathbf{t}'(0,r,0,\epsilon)$, $m'(0,0,r,\epsilon)$, and $n'(\frac{\sqrt{2}}{2}r, \frac{\sqrt{2}}{2}r, 0, r)$. Since $d(s'n')+d(n't') = \frac{1}{2}\pi r$, which is smaller than $d(s'm') + d(m't') = \pi r$, CSR will chose node n to be the relay node for packets between $\mathbf{s}$ and $\mathbf{t}$. The total distance of $\mathbf{P}_{CSR}(\mathbf{s},\mathbf{t}) = \|\mathbf{s}n\| + \|n\mathbf{t}\| = 2\sqrt{(\frac{\sqrt{2}}{2}r-\epsilon)^2 + (\frac{\sqrt{2}}{2}r)^2}$. However, the length of shortest path $\mathbf{P}_{SPR}(\mathbf{s},\mathbf{t}) = \|\mathbf{s}m\| + \|m\mathbf{t}\| = 2\sqrt{2}\epsilon$. Thus, the competitive factor $l = \frac{\mathbf{P}_{CSR}(\mathbf{s},\mathbf{t})}{\mathbf{P}_{SPR}(\mathbf{s},\mathbf{t})} = \sqrt{\frac{(\frac{\sqrt{2}}{2}r-\epsilon)^2+(\frac{\sqrt{2}}{2}r)^2}{2\epsilon^2}}$. When ϵ is arbitrary small, l can be arbitrary large. ■

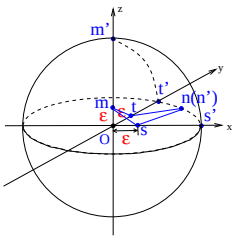

Fig. 3. Proof of unbounded CF for CSR with Projection Method I.

Theorem 1 implies that CSR with Projection Method I may use an arbitrary longer path than the shortest path in the worst case. Fortunately, the worst case seldom occurs in a random network. Later, we will use our simulation results to show that the CF of CSR with Projection Method I is not very large for grid or random networks in practice.

Before proving the competitiveness of CSR with Projection Method II, we present some preliminaries for stereographic projection. Assume that the furthest wireless node is of distance D from the center S of 3D hyperplane. The w' value of the highest projection on the 4D sphere (denoted by k) is $k = w'_{max} = \frac{2rD^2}{D^2+4r^2}$ through some simple calculations. we choose $r = \frac{D}{2\sqrt{\epsilon}}$ ($\epsilon > 0$), thus $k = \frac{2r\epsilon}{(1+\epsilon)}$. Recall that stereographic projection is conformal in any dimension, meaning that circles on the sphere map to circles in the plane, thus the projection of a great circle on the 4D sphere $\mathbb{S}^3$ is also a circle in the hyperplane. Let C' denote the arc of $d(m'n')$ and C be the arc of $d(mn)$ (Fig.4(a)). The next lemma show that $d(m'n')$ (or the Euclidean distance $\|mn\|$ between m and n) is not too much different from $d(mn)$ in the hyperplane.

Lemma 2: Consider any two nodes m and n in the 3D Euclidean Space with their projections m' and n' on the 4D sphere $\mathbb{S}^3$, we have $\|mn\| \le d(mn) \le (1+\epsilon)d(m'n')$ and $d(m'n') \le d(mn) \le \frac{\pi}{2}\|mn\|$.

Proof: First, since the Euclidean distance of two points is always smaller than the distance along any arc passing them, $\|mn\| \le d(mn)$. Thus, we only need to prove $d(mn) \le (1+\epsilon)d(m'n')$ to show $\|mn\| \le (1+\epsilon)d(m'n')$. Note that it is an one-to-one mapping between points on C' and points on C. $\int_{C'} dx' = d(m'n')$, where dx' is a miniature segment on C'. Similarly, $\int_C dx = d(mn)$, where dx is the projection of dx' in the 3D Space. See Fig.4(a) for illustration. $p'q'$ is a tiny segment on C' with length $dx' \to 0$, and $dx' = \|p'q'\|$. The projection of $p'q'$ is pq with the length $dx = \|pq\|$. Denote b as the projection of p' on line segment NS (*i.e.* w axis). The w' value of p' (or b), is denoted by w'_p. Then $\frac{\|Nb\|}{\|NS\|} = \frac{2r-w'_p}{2r}$. When $dx', dx \to 0$, *i.e.*, $pq, p'q' \to 0$, pq and $p'q'$ are in the same plane (the plane defined by nodes N, p and q). Then, due to the similarity of triangles $\triangle Np'b$ and $\triangle NpS$, $\frac{dx'}{dx} = \frac{\|p'q'\|}{\|pq\|} = \frac{\|Np'\|}{\|Np\|} = \frac{\|Nb\|}{\|NS\|} = \frac{2r-w'_p}{2r}$. Because the highest

value of w'_p is k, we have $\frac{dx'}{dx} \geq \frac{2r-k}{2r} = \frac{1}{1+\epsilon}$. Thus, $d(mn) = \int_C dx \leq \int_{C'}(1+\epsilon)dx' = (1+\epsilon)d(m'n')$. This finishes the first half of the lemma.

Note that $\frac{dx'}{dx} = \frac{2r-w'_p}{2r} \leq 1$. Thus, $dx' \leq dx$, and $d(m'n') = \int_{C'} dx' \leq \int_C dx = d(mn)$. We also have $\frac{d(mn)}{\|mn\|} \leq \frac{\pi}{2}$ (since $\frac{d(mn)}{\|mn\|}$ reaches the maximum value of $\frac{\pi}{2}$ when $d(mn)$ is a half circle). Therefore, $d(m'n') \leq d(mn) \leq \frac{\pi}{2}\|mn\|$. This concludes the proof. ■

Now we are ready to prove the theorem about the constant competitive factor of CSR using Projection Method II. There are four paths used in the proof as shown in Fig.4(b): $\mathbf{P}_{\mathcal{SPR}}(\mathbf{s},\mathbf{t})$ represents the shortest path connecting the source $\mathbf{s}$ and the destination $\mathbf{t}$ in the 3D Euclidean space; $\mathbf{P}'_{\mathcal{SPR}}(\mathbf{s},\mathbf{t})$ is the surface path connecting all the projections of each node along $\mathbf{P}_{\mathcal{SPR}}(\mathbf{s},\mathbf{t})$ on the 4D sphere using the circular distance; $\mathbf{P}_{\mathcal{CSR}}(\mathbf{s},\mathbf{t})$ denotes the path found by CSR protocol using Projection Method II in the 3D space; and at last $\mathbf{P}'_{\mathcal{CSR}}(\mathbf{s},\mathbf{t})$ is the surface path connecting all the projections of each node along $\mathbf{P}_{\mathcal{CSR}}(\mathbf{s},\mathbf{t})$ on the 4D sphere. For a path $\mathbf{P}_{\mathcal{A}}$ in 3D space, we define $||\mathbf{P}_{\mathcal{A}}||$ as the summation of the Euclidian distance of each link in $\mathbf{P}_{\mathcal{A}}$. For a path $\mathbf{P}'_{\mathcal{A}}$ on the sphere, we define $||\mathbf{P}'_{\mathcal{A}}||$ as the summation of the length of each arc in $\mathbf{P}'_{\mathcal{A}}$.

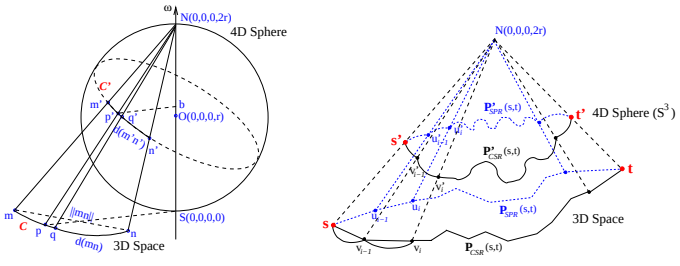

(a) Lemma 2 (b) Theorem 3

Fig. 4. Proof of constant CF for CSR with Projection Method II: the path length of CSR is bounded by the path length of shortest path routing.

Theorem 3: The distance traveled by CSR with projection method II is $\frac{\pi}{2}(1+\epsilon)$-competitive, *i.e.*,

$$||\mathbf{P}_{\mathcal{CSR}}(\mathbf{s},\mathbf{t})|| \leq \frac{\pi}{2}(1+\epsilon)||\mathbf{P}_{\mathcal{SPR}}(\mathbf{s},\mathbf{t})||.$$

Proof: Let $\mathbf{P}_{\mathcal{CSR}}(\mathbf{s},\mathbf{t}) = v_0, v_1, v_2, \cdots, v_n$, where $v_0 = \mathbf{s}$ and $v_n = \mathbf{t}$. Let the projection of $\mathbf{P}_{\mathcal{CSR}}(\mathbf{s},\mathbf{t})$ on the 4D sphere $\mathbf{P}'_{\mathcal{CSR}}(\mathbf{s},\mathbf{t}) = v'_0, v'_1, v'_2, \cdots, v'_n$, where $v'_0 = \mathbf{s}'$ and $v'_n = \mathbf{t}'$. Similarly, let $\mathbf{P}_{\mathcal{SPR}}(\mathbf{s},\mathbf{t}) = u_0, u_1, u_2, \cdots, u_m$, where $u_0 = \mathbf{s} = v_0$ and $u_m = \mathbf{t} = v_n$. Let the projection of $\mathbf{P}_{\mathcal{SPR}}(\mathbf{s},\mathbf{t})$ on the sphere $\mathbf{P}'_{\mathcal{SPR}}(\mathbf{s},\mathbf{t}) = u'_0, u'_1, u'_2, \cdots, u'_m$, where $u'_0 = \mathbf{s}' = v'_0$ and $u'_m = \mathbf{t}' = v'_n$. Note that m may not equal to n.

From Lemma 2, we know $\|v_{i-1}v_i\| \leq (1+\epsilon)d(v'_{i-1}v'_i)$, therefore, $||\mathbf{P}_{\mathcal{CSR}}(\mathbf{s},\mathbf{t})|| = \sum_{i=1}^{n}\|v_{i-1}v_i\| \leq \sum_{i=1}^{n}(1+\epsilon)d(v'_{i-1}v'_i) = (1+\epsilon)||\mathbf{P}'_{\mathcal{CSR}}(\mathbf{s},\mathbf{t})||$. According to CSR protocol, $||\mathbf{P}'_{\mathcal{CSR}}(\mathbf{s},\mathbf{t})|| \leq ||\mathbf{P}'_{\mathcal{SPR}}(\mathbf{s},\mathbf{t})||$ since $\mathbf{P}'_{\mathcal{CSR}}(\mathbf{s},\mathbf{t})$ has the shortest total spherical distance among all routes on the sphere surface connecting $\mathbf{s}'$ and $\mathbf{t}'$. From Lemma 2, we also have $d(u'_{i-1}u'_i) \leq \frac{\pi}{2}\|u_{i-1}u_i\|$. Thus, $||\mathbf{P}'_{\mathcal{SPR}}(\mathbf{s},\mathbf{t})|| = \sum_{i=1}^{n} d(u'_{i-1}u'_i) \leq \sum_{i=1}^{n}\frac{\pi}{2}\|u_{i-1}u_i\| = \frac{\pi}{2}||\mathbf{P}_{\mathcal{SPR}}(\mathbf{s},\mathbf{t})||$. Consequently, $||\mathbf{P}_{\mathcal{CSR}}(\mathbf{s},\mathbf{t})|| \leq (1+\epsilon)||\mathbf{P}'_{\mathcal{CSR}}(\mathbf{s},\mathbf{t})|| \leq (1+\epsilon)||\mathbf{P}'_{\mathcal{SPR}}(\mathbf{s},\mathbf{t})|| \leq \frac{\pi}{2}(1+\epsilon)||\mathbf{P}_{\mathcal{SPR}}(\mathbf{s},\mathbf{t})||$. ■

Theorem 3 gives a theoretical bound of the competitiveness of CSR using Projection Method II. It shows that the path length of CSR is not too much different from the path length of the shortest path routing even in the worst case scenario. Since $\epsilon = \frac{D^2}{4r^2}$, with the adjustable parameter r (*i.e.*, the radius of the sphere), we can control the competitiveness factor easily.

IV. Simulation

We now evaluate the performance of CSR and LCSR via extensive simulations for both 3D grid networks and 3D random networks in a $20 \times 20 \times 20$ cubic area. We compare their performance under the all-to-all communication scenario, *i.e.*, every pair of nodes has unit message to communicate. Hereafter, we use 3D-CSR/3D-LCSR to denote the routing methods with Projection Method I (mapping nodes on a 3D sphere) and 4D-CSR/4D-LCSR to denote the routing methods with Projection Method II (mapping nodes on a 4D sphere).

A. CSR vs SPR:

For grid network, 216 wireless nodes are distributed in 6^3 grids. The transmission range (Tr) is set to 4.5. For 3D random networks, 100 nodes are randomly distributed in the 20^3 cube with each node's Tr set to 6. We run the simulation for 100 random networks and take the average. We try different sizes of the sphere (with radii 3, 5 and 15).

Fig.5 demonstrates the average (Avg), maximum (Max) traffic load, and standard deviation (Std) of load for SPR, 3D-CSR and 4D-CSR with different sphere sizes ($r = 3$, 5 and 15) for the grid and random networks. The leftmost bar of each sub-graph represents the Shortest Path Routing (SPR) method, the red bars represent 3D-CSR and blue bars represent 4D-CSR. The average load of 3D-CSR is larger than SPR. However, 4D-CSR has even smaller average load than SPR especially for random networks. All CSR algorithms have much smaller maximum load and Std of load than SPR, *e.g.*, the maximum load of 4D-CSR ($r = 5$) has decreased about 40.9% compared with SPR (from 1978.0 to 1050.0); and the Std of 3D-CSR ($r = 3$) has about 55.4% deduction compared with SPR (from 423.4 to 188.9). Thus, our simulation results show that CSR can achieve better load balancing than SPR.

We also study the competitiveness factor (CF) of CSR by measuring the CF of each route generated by CSR in our simulation. Table I gives the average and maximum competitiveness factor (Avg CF and Max CF) of CSR with various radii. Remember that 3D-CSR has unbounded CF in theory. As shown in Table I, Max CFs of 3D-CSR ($r = 3$ and 5) for grid networks are around 6.6 which are much larger than the Max CFs of 4D-CSR. From Theorem 3, the distance traveled by 4D-CSR satisfies $||\mathbf{P}_{4\mathcal{D}-\mathcal{CSR}}(\mathbf{s},\mathbf{t})|| \leq \frac{\pi}{2}(1+\epsilon)||\mathbf{P}_{\mathcal{SPR}}(\mathbf{s},\mathbf{t})||$, where $\epsilon = \frac{D^2}{4r^2}$. In our simulation settings, $D = 10\sqrt{2}$. Thus, when $r = 3$, 5 and 15, respectively, CF bounds are 10.3, 4.7 and 1.9. The simulation results of CFs confirm our theoretical bounds of 4D-CSR. Actually the practical CFs are much smaller than the bounds, and very close to 1 (from 1.00 to 1.52). In other words, not only CSR has balanced traffic load but also the distance traveled by the packets is almost the same as the minimum (the distance of the shortest path).

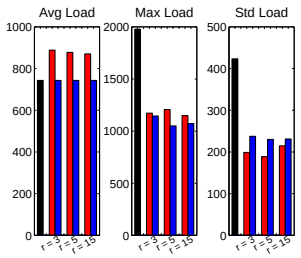

(a) 3D Grid Network

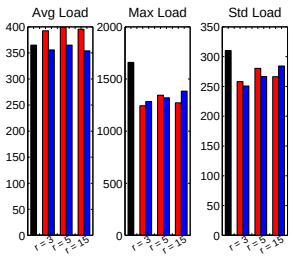

(b) 3D Random Network

Fig. 5. Traffic load comparison among SPR, 3D-CSR and 4D-CSR with radii $r = 3$, 5 and 15: (a) 3D grid network; (b) random networks.

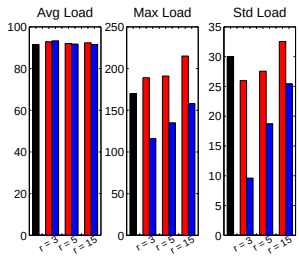

(a) 3D Grid Network

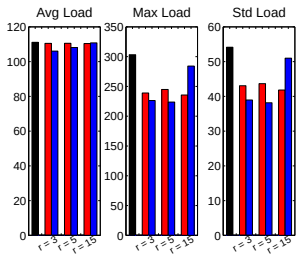

(b) 3D Random Network

Fig. 6. Traffic load comparison among greedy routing, 3D-LCSR and 4D-LCSR with radii $r = 3$, 5 and 15: (a) 3D grid network; (b) random networks.

TABLE I

COMPETITIVENESS FACTOR (CF) OF CSR (VARIOUS SPHERE SIZE)

Network Topology	Radius r	Avg CF		Max CF	
		3D-CSR	4D-CSR	3D-CSR	4D-CSR
Grid	3	1.155	1.011	6.656	1.331
	5	1.143	1.001	6.656	1.171
	15	1.124	1.000	3.828	1.000
Random	3	1.092	1.034	3.077	1.515
	5	1.095	1.021	3.045	1.378
	15	1.097	1.004	2.993	1.216

TABLE II

COMPETITIVENESS FACTOR (CF) AND DELIVERY RATIO OF LCSR

Network Topology	r	Avg/Max CF		Delivery Ratio		
		3D-LCSR	4D-LCSR	Greedy	3D-LCSR	4D-LCSR
Grid	3	1.039/1.589	1.030/1.306	1.00	1.00	1.00
	5	1.031/1.306	1.047/1.306		0.99	1.00
	15	1.036/1.306	1.030/1.306		1.00	1.00
Random	3	1.057/2.700	1.060/3.185	0.98	0.94	0.90
	5	1.051/2.436	1.060/2.431		0.94	0.94
	15	1.049/2.763	1.060/2.486		0.95	0.98

B. LCSR vs Greedy:

We then study the performance of localized version of CSR (denoted by LCSR) via 3D grid and random networks. For grid network, we use a network with 64 nodes in a 4^3 grids and set Tr to 8. For random network, we generate 50 random networks with 64 nodes in a 20^3 cube and set Tr to 8. For the results, we take the average of these 50 networks.

Fig.6 shows the performance comparison of greedy routing, 3D-LCSR and 4D-LCSR for the grid and random networks. The leftmost bar of each sub-graph represents the greedy routing method, red bars represent 3D-LCSR, and blue bars represent 4D-LCSR. For the grid network, 3D-LCSR has larger maximum load than greedy algorithm for all radii, but 4D-LCSR has much better performance than greedy, *i.e.*, almost the same average load with much smaller maximum load and Std of load. For example, the Std of load for 4D-LCSR ($r = 3$) has decreased dramatically from 30.0 to 9.6 (about 68%). In the scenario of random networks, 3D-LCSR and 4D-LCSR both have similar average load to greedy routing, and their maximum load and Std of load are smaller than greedy routing.

We measure the CFs of LCSR compared with greedy routing method. Here, CF is the factor between the distance traveled by packets in LCSR and the distance traveled in greedy routing if both routing methods can find a path between the source and the destination. In our simulation, we randomly select 100 node pairs (*i.e.*, 10 source nodes and 10 destination nodes are randomly chosen) and calculate the CF for each route. Table II provides the results for both grid and random networks. Though we do not have any theoretical bounds for LCSR, the CFs are very small in practice, *i.e.*, ranged from 1.03 to 3.19. This table also gives the delivery ratios. The delivery ratios of 4D- and 3D-LCSR are 100% and almost 100%, respectively for grid network with different radii. For the random networks, the delivery ratios of both 4D- and 3D-LCSR are still very high (more than 90%).

V. CONCLUSION

In this paper, we proposed novel 3D load balancing routing protocols – *3D Circular Sailing Routing* for 3D wireless networks to avoid the uneven load distribution caused by shortest path routing or greedy routing. By spreading the traffic across a virtual sphere, CSR can reduce hot spots of congestion in the network and increase the energy lifetime of the network. CSR can be easily implemented using existing position-based routing protocols without any major changes or additional overhead. In this paper, we not only provided a theoretical proof of the competitiveness of CSR, but also conducted extensive simulations to evaluate the proposed method.

REFERENCES

[1] S.-J. Lee and M. Gerla, "Dynamic load-aware routing in ad hoc networks," in *Proc. of IEEE ICC*, 2001.

[2] H. Hassanein and A. Zhou, "Routing with load balancing in wireless ad hoc networks," in *Proc. of ACM MSWIM*, 2001.

[3] Y. Yoo and S. Ahn, "A simple load-balancing approach in cheat-proof ad hoc networks," in *Proc. of IEEE Globecom*, 2004.

[4] P.P. Pham and S. Perreau, "Performance analysis of reactive shortest path and multipath routing mechanism with load balance," in *Proc. of IEEE INFOCOM*, 2003.

[5] Y. Ganjali and A. Keshavarzian, "Load balancing in ad hoc networks: single-path routing vs. multi-path routing," in *IEEE INFOCOM*, 2004.

[6] E. Hyytia and J. Virtamo, "On traffic load distribution and load balancing in dense wireless multihop networks," *EURASIP Journal on Wireless Communications and Networking*, Article ID 16932, 2007.

[7] L. Popa, A. Rostami, R. Karp, C. Papadimitriou, and I. Stoica, "Balancing the traffic load in wireless networks with curveball routing," in *Proc. of ACM Mobihoc*, 2007.

[8] F. Li and Y. Wang, "Circular Sailing Routing for Wireless Networks," in *Proc. of IEEE Infocom*, 2008.

[9] H. S. M. Coxeter, *Introduction to Geometry*, John Wiley & Sons, New York, 2nd edition, 1969.